Inorganic Chemistry

pubs.acs.org/IC

Communication

# Size-Selective Suzuki–Miyaura Coupling Reaction over Ultrafine Pd Nanocatalysts in a Water-Stable Indium–Organic Framework

Dandan Chen,[†] Linsha Wei,[†] Yihan Yu, Lei Zhao, Qiuhong Sun, Cheng Han, Jianmei Lu,* Huagui Nie, Li-Xiong Shao, Jinjie Qian,* and Zhi Yang*

Cite This: *Inorg. Chem.* 2022, 61, 15320–15324

Read Online



**ABSTRACT:** Metal nanoparticles stabilized by crystalline metal–organic frameworks (MOFs) are highly promising for green heterogeneous catalysis. In this work, *in situ* formed ultrafine Pd nanocatalysts with an average size of 3.14 nm have been successfully immobilized into the mesopores or defects of a water-stable indium-based MOF by the double-solvent method and subsequent reduction. Significantly, the obtained Pd@InOF-1 displays an obvious and satisfactory size-selective effect in the Suzuki–Miyaura coupling reaction between arylboronic acids and aryl bromides. On the basis of the synergistic effect, microporous InOF-1 nanorods afford a confined space for improving the selectivity of target products while Pd nanoparticles endow abundant active sites for catalysis. Herein, choosing the smallest size reactant with only one benzene ring gives the highest isolated yield of 90%, and if the size is larger, the yield is obviously reduced or even the target product could not be collected. Looking forward, this demonstrated study not only assembles a well-designed Pd@MOF composite with unique micro-nanostructures but also delivers an impressive option for cross-coupling reaction, which has implications for the further development of MOF hybrids for sustainable applications.



The formation of carbon–carbon bonds has long been regraded as one of the most prevalent and challenging methodologies in synthetic organic chemistry.[1,2] Among these strategies, Suzuki–Miyaura cross-coupling is recognized as the protagonist for the facile preparation of various asymmetric and symmetric biphenyl compounds that shows great significance in practical pharmaceutical applications.[3−5] In principle, the above

**Scheme 1**[a]

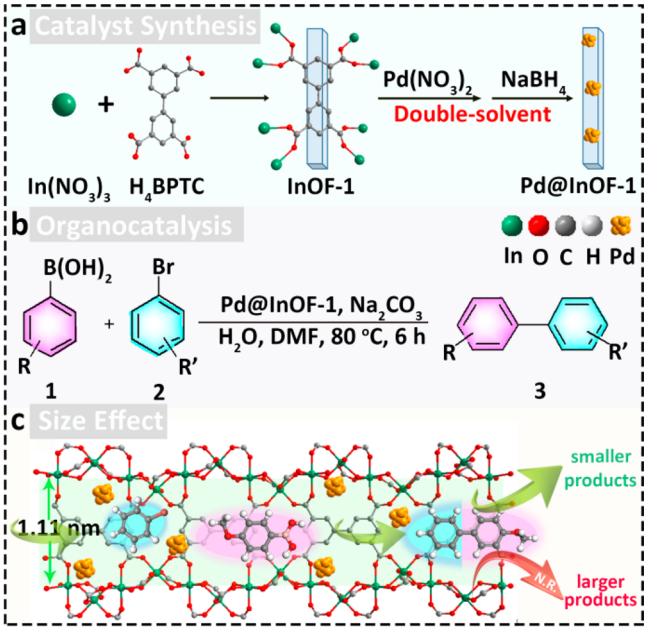


[a](a) Synthetic route for Pd@InOF-1 composite, (b) reactions of arylboronic acids (**1**) and arylbromides (**2**) with Pd@InOF-1, and (c) diagram of size effect catalyzed by Pd@InOF-1.

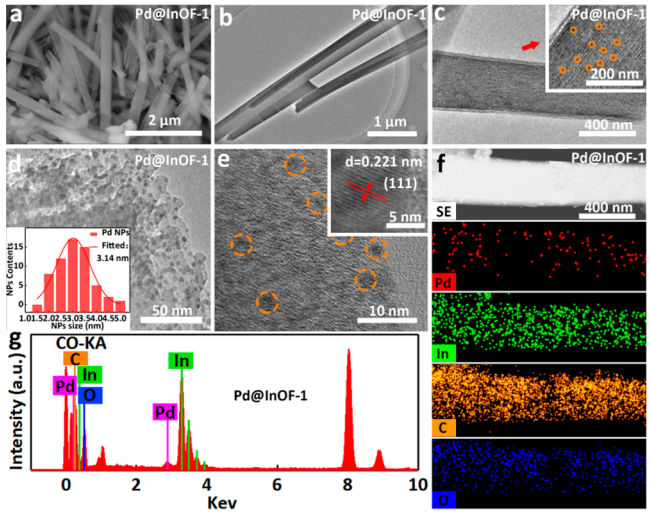


**Figure 1.** (a) SEM, (b) TEM, and (c–e) HR-TEM images, (f) HAADF-STEM and element mapping images, and (g) EDS pattern of Pd@InOF-1.

**Received:** August 10, 2022
**Published:** September 22, 2022

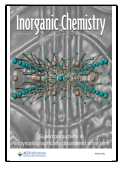




https://doi.org/10.1021/acs.inorgchem.2c02877
*Inorg. Chem.* 2022, 61, 15320–15324

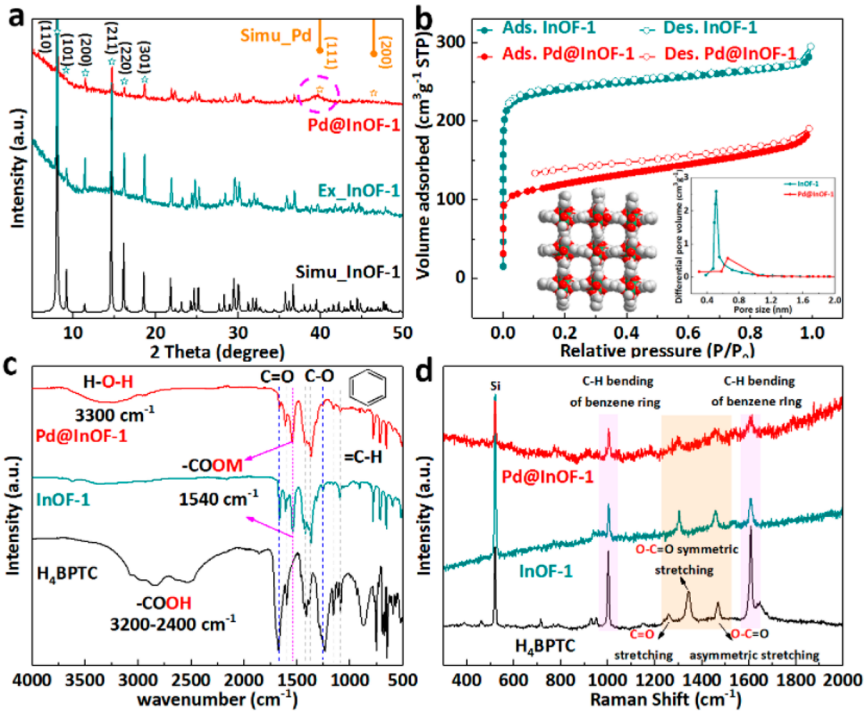


**Figure 2.** (a) PXRD patterns, (b) $N_2$ isotherms and corresponding PSD curves, (c) FT-IR spectra, and (d) Raman spectra of Pd@InOF-1.

coupling reaction proceeds conveniently with the addition of metal catalysts, among which palladium (Pd) is the most commonly used due to its high activity.[6,7] With this method, attaching Pd species to a heterogeneous carrier yields a catalyst that combines the advantages of homogeneous catalysis (catalytically active sites) and sustainable heterogeneous catalysis (high stability and convenient separation). Although many reports on Suzuki−Miyaura coupling over diverse Pd-based heterogeneous nanomaterials have been unveiled,[8−10] there is no report on well-designed catalysts with size-selective reaction to date.[11] Meanwhile, it is worth mentioning that the Pd-based catalyst for the Suzuki−Miyaura coupling should be water-resistant in aqueous systems for better recovery and reuse.[12]

On the other hand, metal−organic frameworks (MOFs), as an emerging subclass of porous hybrids, are self-assembled from inorganic metal centers with versatile organic linkers.[13,14] Multifunctional MOF materials are very appealing as a result of their large porosity, high specific surface area, diversified functionality, and tailorable structural chemistry.[15−17] MOFs have been well demonstrated to be utilized in efficient catalysis when they are combined with external catalysts.[18−25] However, employing microporous MOFs as robust host materials to afford a confined space where the limited growth of ultrafine metal particles can be achieved under certain conditions.[26,27] These well-dispersed metal nanoparticles (NPs) precisely encapsulated inside large MOF pores are a potential platform for heterogeneous catalysis with high selectivity. Inspired by this, it is found that MOFs assembled with high-valent metals, such as In(III) and Zr(IV),[28] can greatly improve the structural stability in aqueous solutions, which are obviously favorable when employed as a robust host for heterogeneous catalysis.

Herein, one type of water-stable InOF-1 is reasonably selected to yield Pd NPs immobilized within tetragonal pores of 1.11 nm,[29] which can be effectively obtained by the solvothermal method. In its single-crystal structure, each deprotonated $BPTC^{4-}$ spacer uses four carboxylates to connect to eight independent In(III) nodes, which are 6-coordinated by four carboxylate oxygen atoms and two oxygen atoms from $\mu_2$-$H_2O$ to form one-dimensional indium−oxygen chains (Figure S1, Table S1). It exhibits excellent structural stability when exposed to the atmosphere and immersed in distilled water and even in boiling water as verified by powder X-ray diffraction (PXRD) (Figure S2). After activation, these desolvated MOF nanorods are well dispersed into a hydrophobic solvent (*n*-hexane) by ultrasonication, then a relatively small volume of hydrophilic solvent (deionized water) dissolved with $Pd(NO_3)_2$ is further dropped into the above *n*-hexane solution.[30] In this case, the restricted volume of the Pd solution could be fully drawn into presynthesized InOF-1 channels through capillary force. Followed by subsequent reduction with sodium borohydride ($NaBH_4$), it would result in the *in situ* growth of ultrafine Pd particles into MOF nanopores or defects created during the metalation process, denoted as Pd@InOF-1 (Scheme 1a, Figures S3 and S4). In Scheme 1b and c, a series of Suzuki−Miyaura reactions have been logically investigated using this Pd@InOF-1, which reveals obvious catalytic activity according to the highly efficient size selectivity. The microstructure and morphology of the as-obtained Pd@InOF-1 composite are first characterized by scanning electron microscopy (SEM) and transmission electron microscopy (TEM). It is worth mentioning that the employment of a palladium source during the preparation of Pd@InOF-1 does not cause serious corrosion, which retains the highly crystalline nanotube with a smooth external surface similar to that of its precursor (Figures 1a,b and S5). Interestingly, ultrafine Pd particles are uniformly encapsulated inside the MOF as seen in the high-resolution TEM (HR-TEM) images (Figures 1c and S6), certifying the spatial confinement effect.[31−33] It can be clearly observed that these Pd species display an average diameter of 3.14 nm, while some identifiable lattice fringe spacings of 0.221 nm are ascribed to the (111) plane of metallic Pd in Figure 1d,e. Furthermore, high-


https://doi.org/10.1021/acs.inorgchem.2c02877
Inorg. Chem. 2022, 61, 15320−15324

**Table 1. Suzuki–Miyaura Coupling Reaction Catalyzed by Pd@InOF-1**

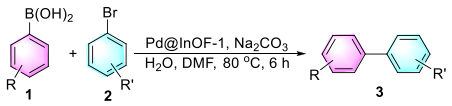


| Entry[a] | 1 | 2 | Yield (%)[b] |
|---|---|---|---|
| 1 | 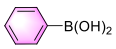 1e |  2a | **3a**, 94 |
| 2 | 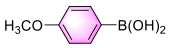 1a |  2a | **3b**, 90 |
| 3 |  1e | 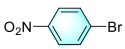 2e | **3c**, 77 |
| 4 | 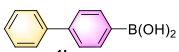 1b |  2a | **3d**, 62 |
| 5 |  1c |  2a | **3e**, 41 |
| 6 | 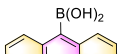 1d |  2a | 0 |
| 7 | 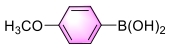 1a | 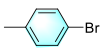 2d | **3f**, 91 |
| 8 |  1a |  2b | **3g**, 37 |
| 9 |  1a |  2c | **3h**, 26 |
| 10 | 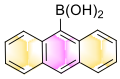 1d |  2c | 0 |

[a]Under $N_2$, all reactions were carried out using arylboronic acids **1** (1.2 mmol), aryl bromides **2** (1.0 mmol), $Na_2CO_3$ (2.0 mmol), Pd@InOF-1 (10.0 mg) in $H_2O$/DMF (2.0 mL/1.0 mL) at 80 °C for 6 h. [b]Isolated yields.

angle annular dark-field scanning TEM (HAADF-STEM) and its corresponding mapping images reveal the uniform distribution of Pd, In, C, and O atoms, and energy-dispersive X-ray spectroscopy (EDS) also confirms coexistence of these four elements (Figure 1f,g). In this case, these *in situ* formed Pd NPs embedded into nanosized MOF pores are featured with abundant catalytic sites for heterogeneous catalysis.

In order to verify the structural components of composites, PXRD is used to show two sets of peaks attributed to the tetragonal phase of InOF-1 and face-centered-cubic phase of Pd (PDF#65-2867), respectively (Figure 2a). In detail, the unchanged peak positions with reduced intensity indicate the successful integration of porous MOF and Pd species where one moderate peak at ∼40° belongs to the (111) plane of Pd.[34] In Figure 2b, similar Type-I isotherms are observed, and their pore size distribution (PSD) curves exhibit a maximum distribution of ∼0.51 and ∼0.66 nm for InOF-1 and Pd@InOF-1, respectively. The calculated specific surface areas are 724.32 and 380.51 $m^2\ g^{-1}$ for pure InOF-1 and Pd@InOF-1, respectively, indicating that the obtained Pd species would partially block MOF channels (Table S2). The Pd ratio in Pd@InOF-1 has been tested by ICP-MS (Table S3). Furthermore, FT-IR analysis reveals the aromatic ring skeleton vibration (Figure 2c), where two peaks of 1676 and 1256 $cm^{-1}$ correspond to the O=C and C–O stretching from organic ligands. In particular, the main differences in 3200–2400 $cm^{-1}$ are assigned to the O–H stretching, and a peak at 1540 $cm^{-1}$ is assigned to coordination bonds. Meanwhile, two bands at 1004 and 1605 $cm^{-1}$ come from symmetric C–H bending vibrations of biphenyl-3,3′,5,5′-tetracarboxylic acid ($H_4$BPTC) in the Raman spectra (Figure 2d). Compared to InOF-1 and Pd@InOF-1, the C=O stretching (1258 $cm^{-1}$), C–O symmetric (1340 $cm^{-1}$), and asymmetric (1470 $cm^{-1}$) vibration peaks shift to lower wavenumbers after coordination.[35,36] The discussion above confirms the robust structural stability of Pd@InOF-1 after loading fine metal NPs, which lays the foundation for the following size-selective catalysis.

A series of reactions between different arylboronic acids and aryl bromides are performed to evaluate the catalytic performance of Pd@InOF-1 in terms of size effect.[37−40] After optimizing solvent conditions, the optimal reaction is conducted in a mixture of solvents of DMF and $H_2O$ using $Na_2CO_3$ as the base (Table S4). First, no reaction occurs in the system without additive and in the case of only pure MOF without Pd (Table S5). Second, using the smallest sized phenyl boronic acid **1e** as a substrate to react with bromobenzene **2a**, the biphenyl **3a** product is collected in the highest isolated yields of 94% (Entry 1) with high selectivity in Tables 1 and S6. With bromobenzene **2a** as the reactant, its reaction with 4-methoxyphenylboronic acid **1a** gives an isolated yield of the desired product (**3b**, 90%, Entry 2). In addition, bromobenzene **2a** with electron withdrawing 1-bromo-4-nitrobenzene **2e** could produce the desired product in 77% yield on account of the inhibition of strong electron withdrawing groups and size effect of the substrate (**3c**, Entry 3). Third, 4-biphenylboronic acid **1b** can also be activated with a moderate yield of 62% (**3d**, Entry 4); while using 1-naphthaleneboronic acid **1c**, the yield is reduced to be 41% (**3e**, Entry 5). Under the same conditions, the target product could not be collected using 9-anthraceneboronic acid **1d** (Entry 6). Fourth, various aryl bromides are also examined to attest the size effect of the Pd@InOF-1 catalyst, in which the combination of 1-bromo-4-methylbenzene **2d** and 4-methoxyphenylboronic acid **1a** provides a reasonable yield of 91% (**3f**, Entry 7). When using 4-methoxyphenylboronic acid **1a** as a substrate to react with 1-bromo-2-methylbenzene **2b**, the product (**3g**, Entry 8) is collected in 37% yield, demonstrating that the steric effect of aryl bromides is sensitive to the reaction. When using 1-bromonaphthalene **2c** and 4-methoxyphenylboronic acid **1a** as the reactants, it shows the desired product with 26% yield (**3h**, Entry 9). Similarly, 9-anthraceneboronic acid **1d** and 1-bromonaphthalene **2c** are not able to produce the desired product on account of the severe spatial hindrance (Entry 10). Furthermore, the influence of the concentration of Pd on the catalysts was also examined (Table S5). The synthesized Pd@InOF-1-L endows few Pd species and low activity with a retained morphology as well as preserved crystallinity, while the overall framework of Pd@InOF-1-H is mostly destroyed as shown in Figure S7. The prominent peak of Pd is detected by XRD,


https://doi.org/10.1021/acs.inorgchem.2c02877
Inorg. Chem. 2022, 61, 15320−15324

indicating severe Pd particle aggregation in Pd@InOF-1-H, and is not suitable for size-selective catalysis (Figure S8). For more detailed synthetic products and their NMR data with high size-selective efficiency, please see Figures S9−S17 and Table S7. All the sizes of the optimized molecular structures are calculated from Materials Studio, unless otherwise mentioned (Figures S18−S29).

In summary, crystalline and robust InOF-1 nanorods with large tetragonal channels are employed to confine Pd particles with an average size of 3.14 nm on account of a double-solvent method followed by $NaBH_4$ reduction. The obtained Pd@InOF-1 composite behaves as a highly size-selective catalyst and reveals excellent performance in the Suzuki−Miyaura coupling reaction. Based on the above discussion, several conclusions can be made as follows: (i) The parent InOF-1 shows no catalytic activity, which only endows the nanosized channels for *in situ* formed Pd NPs. (ii) The as-synthesized Pd@InOF-1 exhibits an obvious size effect for the coupling reaction. (iii) Small-sized reactants (two or fewer benzene rings) including aryl bromides or arylboronic acids can smoothly and freely come in and out of the nanochannels to give the corresponding smaller products in relatively higher yields, while large-sized reactants have greater steric hindrance, giving the products in lower yields even though no reaction occurred. The facile synthesis and rational design as well as satisfactory selectivity of Pd@InOF-1 in this work might pave new paths to MOF-based composites for wide applications in heterogeneous catalysis in the near future.

## ■ ASSOCIATED CONTENT

### Supporting Information

The Supporting Information is available free of charge at https://pubs.acs.org/doi/10.1021/acs.inorgchem.2c02877.

Experimental details; PXRD patterns; SEM and TEM images; $^1$H NMR spectra; molecular structures; X-ray data (PDF)

## ■ AUTHOR INFORMATION


### Corresponding Authors

**Jianmei Lu** − *Key Laboratory of Carbon Materials of Zhejiang Province, College of Chemistry and Materials Engineering, Wenzhou University, Wenzhou, Zhejiang 325035, P. R. China*; orcid.org/0000-0002-6983-9846; Email: ljm@wzu.edu.cn

**Jinjie Qian** − *Key Laboratory of Carbon Materials of Zhejiang Province, College of Chemistry and Materials Engineering, Wenzhou University, Wenzhou, Zhejiang 325035, P. R. China*; orcid.org/0000-0002-9996-7929; Email: jinjieqian@wzu.edu.cn

**Zhi Yang** − *Key Laboratory of Carbon Materials of Zhejiang Province, College of Chemistry and Materials Engineering, Wenzhou University, Wenzhou, Zhejiang 325035, P. R. China*; Email: yangzhi@wzu.edu.cn

### Authors

**Dandan Chen** − *Key Laboratory of Carbon Materials of Zhejiang Province, College of Chemistry and Materials Engineering, Wenzhou University, Wenzhou, Zhejiang 325035, P. R. China*

**Linsha Wei** − *Key Laboratory of Carbon Materials of Zhejiang Province, College of Chemistry and Materials Engineering, Wenzhou University, Wenzhou, Zhejiang 325035, P. R. China*

**Yihan Yu** − *Key Laboratory of Carbon Materials of Zhejiang Province, College of Chemistry and Materials Engineering, Wenzhou University, Wenzhou, Zhejiang 325035, P. R. China*

**Lei Zhao** − *Key Laboratory of Carbon Materials of Zhejiang Province, College of Chemistry and Materials Engineering, Wenzhou University, Wenzhou, Zhejiang 325035, P. R. China*

**Qiuhong Sun** − *Key Laboratory of Carbon Materials of Zhejiang Province, College of Chemistry and Materials Engineering, Wenzhou University, Wenzhou, Zhejiang 325035, P. R. China*

**Cheng Han** − *Key Laboratory of Carbon Materials of Zhejiang Province, College of Chemistry and Materials Engineering, Wenzhou University, Wenzhou, Zhejiang 325035, P. R. China*

**Huagui Nie** − *Key Laboratory of Carbon Materials of Zhejiang Province, College of Chemistry and Materials Engineering, Wenzhou University, Wenzhou, Zhejiang 325035, P. R. China*

**Li-Xiong Shao** − *Key Laboratory of Carbon Materials of Zhejiang Province, College of Chemistry and Materials Engineering, Wenzhou University, Wenzhou, Zhejiang 325035, P. R. China*; orcid.org/0000-0002-7589-1800

Complete contact information is available at: https://pubs.acs.org/10.1021/acs.inorgchem.2c02877


### Author Contributions

†D.C. and L.W. contributed equally to this work. and both of them conducted the major experiments and performed the characterizations. J.Q. conceived the research project. D.C. and L.W. conducted the experiments and performed the characterizations. J.Q. and D.C. wrote the manuscript with the input from the other authors. All authors have given approval to the final version of the manuscript.

### Notes

The authors declare no competing financial interest.

## ■ ACKNOWLEDGMENTS

This work was financially supported by National Natural Science Foundation of China (21601137), Natural Science Foundation of Zhejiang Province (LQ16B010003), Basic Science and Technology Research Project of Wenzhou, Zhejiang Province (G20190007), and the Special Basic Cooperative Research Programs of Yunnan Provincial Undergraduate Universities Association (202101BA070001-042).

## ■ REFERENCES


(1) Eppe, G.; Didier, D.; Marek, I. Stereocontrolled formation of several carbon-carbon bonds in acyclic systems. *Chem. Rev.* **2015**, *115*, 9175−9206.

(2) Just-Baringo, X.; Larrosa, I. Ketone C-C bond activation meets the Suzuki-Miyaura cross-coupling. *Chem.* **2018**, *4*, 1203−1204.

(3) Meng, G.; Shi, S.; Szostak, M. Palladium-catalyzed Suzuki-Miyaura cross-coupling of amides via site-selective N-C bond cleavage by cooperative catalysis. *ACS Catal.* **2016**, *6*, 7335−7339.

(4) Niwa, T.; Uetake, Y.; Isoda, M.; Takimoto, T.; Nakaoka, M.; Hashizume, D.; Sakurai, H.; Hosoya, T. Lewis acid-mediated Suzuki-Miyaura cross-coupling reaction. *Nat. Catal.* **2021**, *4*, 1080−1088.

(5) Pascanu, V.; Hansen, P. R.; Gómez, A. B.; Ayats, C.; Platero-Prats, A. E.; Johansson, M. J.; Pericàs, M. À.; Martín-Matute, B. Highly functionalized biaryls via Suzuki-Miyaura cross-coupling catalyzed by

Pd@MOF under batch and continuous flow regimes. *ChemSusChem* **2015**, *8*, 123−130.
(6) Jansa, J.; Řezníček, T.; Jambor, R.; Bureš, F.; Lyčka, A. Synthesis of hydroxy-substituted *p*-terphenyls and some larger oligophenylenes via palladium on charcoal catalyzed Suzuki-Miyaura reaction. *Adv. Synth. Catal.* **2017**, *359*, 339−350.
(7) Zhu, Q.-L.; Song, F.-Z.; Wang, Q.-J.; Tsumori, N.; Himeda, Y.; Autrey, T.; Xu, Q. A solvent-switched in situ confinement approach for immobilizing highly-active ultrafine palladium nanoparticles: boosting catalytic hydrogen evolution. *J. Mater. Chem. A* **2018**, *6*, 5544−5549.
(8) Li, X.; Zhang, B.; Van Zeeland, R.; Tang, L.; Pei, Y.; Qi, Z.; Goh, T. W.; Stanley, L. M.; Huang, W. Unveiling the effects of linker substitution in Suzuki coupling with palladium nanoparticles in metal-organic frameworks. *Catal. Lett.* **2018**, *148*, 940−945.
(9) Yuan, B.; Pan, Y.; Li, Y.; Yin, B.; Jiang, H. Highly active heterogeneous palladium catalyst for the Suzuki-Miyaura and Ullmann coupling reactions of aryl chlorides in aqueous media. *Angew. Chem., Int. Ed.* **2010**, *49*, 4054−4058.
(10) You, L.-X.; Zhao, B.-B.; Yao, S.-X.; Xiong, G.; Dragutan, I.; Dragutan, V.; Ding, F.; Sun, Y.-G. Engineering functional group decorated ZIFs to high-performance Pd@ZIF-92 nanocatalysts for $C(sp^2)$-$C(sp^2)$ couplings in aqueous medium. *J. Catal.* **2020**, *392*, 80−87.
(11) Chen, W. M.; Cai, P. Y.; Elumalai, P.; Zhang, P.; Feng, L.; Al-Rawashdeh, M.; Madrahimov, S. T.; Zhou, H.-C. Site-isolated azobenzene-containing metal-organic framework for cyclopalladated catalyzed Suzuki-Miyuara coupling in flow. *ACS Appl. Mater. Interfaces* **2021**, *13*, 51849−51854.
(12) Roglans, A.; Pla-Quintana, A.; Moreno-Mañas, M. M. Diazonium salts as substrates in palladium-catalyzed cross-coupling reactions. *Chem. Rev.* **2006**, *106*, 4622−4643.
(13) Zhong, L.; Ding, J.; Qian, J.; Hong, M. Unconventional inorganic precursors determine the growth of metal-organic frameworks. *Coord. Chem. Rev.* **2021**, *434*, 213804.
(14) Wang, K.; Li, Y.; Xie, L.-H.; Li, X.; Li, J.-R. Construction and application of base-stable MOFs: a critical review. *Chem. Soc. Rev.* **2022**, *51*, 6417.
(15) Zhang, X.; Fan, Y.; You, E.; Li, Z.; Dong, Y.; Chen, L.; Yang, Y.; Xie, Z.; Kuang, Q.; Zheng, L. MOF encapsulated sub-nm Pd skin/Au nanoparticles as antenna-reactor plasmonic catalyst for light driven $CO_2$ hydrogenation. *Nano Energy* **2021**, *84*, 105950.
(16) Zhu, Q.-L.; Xu, Q. Immobilization of ultrafine metal nanoparticles to high-surface-area materials and their catalytic applications. *Chem.* **2016**, *1*, 220−245.
(17) Wu, Y.-L.; Li, X. F.; Wei, Y.-S.; Fu, Z. M.; Wei, W. B.; Wu, X.-T.; Zhu, Q.-L.; Xu, Q. Ordered macroporous superstructure of nitrogen-doped nanoporous carbon implanted with ultrafine Ru nanoclusters for efficient pH-universal hydrogen evolution reaction. *Adv. Mater.* **2021**, *33*, 2006965.
(18) Bok, J.; Lee, S. Y.; Lee, B.-H.; Kim, C.; Nguyen, D. L. T.; Kim, J. W.; Jung, E.; Lee, C. W.; Jung, Y.; Lee, H. S.; Kim, J.; Lee, K.; Ko, W.; Kim, Y. S.; Cho, S.-P.; Yoo, J. S.; Hyeon, T.; Hwang, Y. J. Designing atomically dispersed Au on tensile-strained Pd for efficient $CO_2$ electroreduction to formate. *J. Am. Chem. Soc.* **2021**, *143* (14), 5386−5395.
(19) Chen, D.; Yang, W.; Jiao, L.; Li, L.; Yu, S.-H.; Jiang, H.-L. Boosting catalysis of Pd nanoparticles in MOFs by pore wall engineering: the roles of electron transfer and adsorption energy. *Adv. Mater.* **2020**, *32*, 2000041.
(20) Wang, X.; Dong, A.; Hu, Y.; Qian, J.; Huang, S. A review of recent work on using metal-organic frameworks to grow carbon nanotubes. *Chem. Commun.* **2020**, *56*, 10809−10823.
(21) Chai, L.; Hu, Z.; Wang, X.; Zhang, L.; Li, T.; Hu, Y.; Pan, J.; Qian, J.; Huang, S. $Fe_7C_3$ nanoparticles with in situ grown CNT on nitrogen doped hollow carbon cube with greatly enhanced conductivity and ORR performance for alkaline fuel cell. *Carbon* **2021**, *174*, 531−539.
(22) Xu, M.; Li, D.; Sun, K.; Jiao, L.; Xie, C.; Ding, C.; Jiang, H.-L. Interfacial microenvironment modulation boosting electron transfer between metal nanoparticles and MOFs for enhanced photocatalysis. *Angew. Chem., Int. Ed.* **2021**, *60*, 16372−16376.
(23) Peng, L.; Yang, S.; Jawahery, S.; Moosavi, S. M.; Huckaba, A. J.; Asgari, M.; Oveisi, E.; Nazeeruddin, M. K.; Smit, B.; Queen, W. L. Preserving porosity of mesoporous metal-organic frameworks through the introduction of polymer guests. *J. Am. Chem. Soc.* **2019**, *141*, 12397−12405.
(24) Guo, Y.; Huang, Q.; Ding, J.; Zhong, L.; Li, T.; Pan, J.; Hu, Y.; Qian, J.; Huang, S. CoMo carbide/nitride from bimetallic MOF precursors for enhanced OER performance. *Int. J. Hydrogen Energy* **2021**, *46*, 22268−22276.
(25) Chen, L.-W.; Hao, Y.-C.; Guo, Y.; Zhang, Q.; Li, J.; Gao, W.-Y.; Ren, L.; Su, X.; Hu, L.; Zhang, N.; Li, S.; Feng, X.; Gu, L.; Zhang, Y.-W.; Yin, A.-X.; Wang, B. Metal-organic framework membranes encapsulating gold nanoparticles for direct plasmonic photocatalytic nitrogen fixation. *J. Am. Chem. Soc.* **2021**, *143*, 5727−5736.
(26) Yang, Q.; Xu, Q.; Jiang, H.-L. Metal-organic frameworks meet metal nanoparticles: synergistic effect for enhanced catalysis. *Chem. Soc. Rev.* **2017**, *46*, 4774−4808.
(27) Zhu, Q.-L.; Li, J.; Xu, Q. Immobilizing metal nanoparticles to metal-organic frameworks with size and location control for optimizing catalytic performance. *J. Am. Chem. Soc.* **2013**, *135*, 10210−10213.
(28) Jiang, H.; Yang, K.; Zhao, X.; Zhang, W.; Liu, Y.; Jiang, J.; Cui, Y. Highly stable Zr(IV)-based metal-organic frameworks for chiral separation in reversed-phase liquid chromatography. *J. Am. Chem. Soc.* **2021**, *143*, 390−398.
(29) Qian, J.; Jiang, F.; Yuan, D.; Wu, M.; Zhang, S.; Zhang, L.; Hong, M. Highly selective carbon dioxide adsorption in a water-stable indium-organic framework material. *Chem. Commun.* **2012**, *48*, 9696−9698.
(30) Yu, J.; Mu, C.; Yan, B.; Qin, X.; Shen, C.; Xue, H.; Pang, H. Nanoparticle/MOF composites: preparations and applications. *Mater. Horiz.* **2017**, *4*, 557−569.
(31) Wu, S.-M.; Yang, X.-Y.; Janiak, C. Confinement effects in zeolite-confined noble metals. *Angew. Chem. Int. Ed.* **2019**, *58*, 12340−12354.
(32) Guo, F.; Yang, S.; Liu, Y.; Wang, P.; Huang, J.; Sun, W.-Y. Size engineering of metal-organic framework MIL-101(Cr)-Ag hybrids for photocatalytic $CO_2$ reduction. *ACS Catal.* **2019**, *9*, 8464−8470.
(33) Zhang, X.; Kitao, T.; Piga, D.; Hongu, R.; Bracco, S.; Comotti, A.; Sozzani, P.; Uemura, T. Carbonization of single polyacrylonitrile chains in coordination nanospaces. *Chem. Sci.* **2020**, *11*, 10844−10849.
(34) Mao, Y.; Shi, Y.; Su, Y.; Shen, Q.; Zhang, Y.; Wang, X.; Wen, X. Synthesis of a task-specific imidazolium-based porous triazine polymer decorated with ultrafine Pd nanoparticles toward alcohol oxidation. *Green Chem.* **2021**, *23*, 5981−5989.
(35) Zha, Q.; Li, M.; Liu, Z.; Ni, Y. Hierarchical Co,Fe-MOF-74/Co/carbon cloth hybrid electrode: simple construction and enhanced catalytic performance in full water splitting. *ACS Sustainable Chem. Eng.* **2020**, *8*, 12025−12035.
(36) Deng, M.; Pan, Y.; Zhu, J.; Chen, Z.; Sun, Z.; Sun, J.; Ling, Y.; Zhou, Y.; Feng, P. Cation-exchange approach to tuning the flexibility of a metal-organic framework for gated adsorption. *Inorg. Chem.* **2017**, *56*, 5069−5075.
(37) Fan, H.; Qi, Z.; Sui, D.; Mao, F.; Chen, R.; Huang, J. Palladium nanoparticles in cross-linked polyaniline as highly efficient catalysts for Suzuki-Miyaura reactions. *Chin. J. Catal.* **2017**, *38*, 589−596.
(38) Lei, Y.; Wan, Y.; Li, G.; Zhou, X.-Y.; Gu, Y.; Feng, J.; Wang, R. Palladium supported on an amphiphilic porous organic polymer: a highly efficient catalyst for aminocarbonylation reactions in water. *Mater. Chem. Front.* **2017**, *1*, 1541−1549.
(39) Kim, S.; Jee, S.; Choi, K. M.; Shin, D.-S. Single-atom Pd catalyst anchored on Zr-based metal-organic polyhedra for Suzuki-Miyaura cross coupling reactions in aqueous media. *Nano Res.* **2021**, *14*, 486−492.
(40) Mäsing, F.; Nüsse, H.; Klingauf, J.; Studer, A. Visible-light-enabled preparation of palladium nanoparticles and application as catalysts for Suzuki-Miyaura coupling. *Org. Lett.* **2018**, *20*, 752−755.